Research Square

Preprints are preliminary reports that have not undergone peer review.
They should not be considered conclusive, used to inform clinical practice,
or referenced by the media as validated information.

Genome-wide analysis of the SABATH gene family and functional characterization of SiSABATH9 as a cold-responsive candidate gene in Sesamum indicum L

Xinpai Qiao
Oil Crops Research Institute, Chinese Academy of Agricultural Sciences
Xianmei Hu
Oil Crops Research Institute, Chinese Academy of Agricultural Sciences
Yuhan Wang
Oil Crops Research Institute, Chinese Academy of Agricultural Sciences
Lihua Fan
School of Life Science, Hubei University
Linhai Wang
Oil Crops Research Institute, Chinese Academy of Agricultural Sciences
Huan Li
Oil Crops Research Institute, Chinese Academy of Agricultural Sciences
Jun You
Oil Crops Research Institute, Chinese Academy of Agricultural Sciences
Yanxin Zhang
Oil Crops Research Institute, Chinese Academy of Agricultural Sciences
Li Yang
yangli06@caas.cn

Oil Crops Research Institute, Chinese Academy of Agricultural Sciences

Research Article

Keywords: SABATH gene family, sesame (Sesamum indicum L.), low-temperature stress, methyltransferase, SiSABATH9

Posted Date: November 20th, 2026

DOI: https://doi.org/10.21203/rs.3.rs-11606280/v1

License: This work is licensed under a Creative Commons Attribution 4.0 International License.
Read Full License

Additional Declarations: No competing interests reported.

Genome-wide analysis of the *SABATH* gene family and functional characterization of *SiSABATH9* as a cold-responsive candidate gene in *Sesamum indicum* L.

Xinpai Qiao[1], Xianmei Hu[1], Yuhan Wang[1], Lihua Fan[3], Linhai Wang[1], Huan Li[1], Jun You[1], Yanxin Zhang[1,2]*, and Li Yang[1]*

[1]Oil Crops Research Institute, Chinese Academy of Agricultural Sciences/ Key Laboratory of Biology and Improvement of Oil Crops, Ministry of Agriculture and Rural Affairs, Wuhan 430062, China;

[2]National Salt-Alkali Land Comprehensive Utilization Technology Innovation Center, Dongying 257345, China

[3]School of Life Science, Hubei University, Wuhan 430062, Hubei, China

*Correspondence: yangli06@caas.cn (L.Y.) and zhangyanxin@caas.cn (Y.Z.)

Abstract

Background: The *SABATH* gene family encodes plant-specific S-adenosyl-L-methionine-dependent methyltransferases involved in the methylation of phytohormones and other signaling metabolites. However, this family has not been systematically characterized in sesame (*Sesamum indicum* L.), and its potential roles in abiotic stress, especially in low-temperature stress remain poorly understood.

Results: In this study, 31 *SiSABATH* genes were identified in the sesame genome and exhibited substantial variation in chromosomal distribution, coding-sequence characteristics, conserved motifs, promoter architecture, and tissue-specific expression. Phylogenetic analysis assigned the SiSABATH proteins to Groups I, III, IV, and VI, with Group I containing the largest number of sesame members. Promoter analysis revealed abundant hormone- and stress-responsive cis-acting elements, including Low-temperature-responsive LTR elements in

12 *SiSABATH* genes. Expression profiling under low-temperature treatment further demonstrated pronounced temporal and genotype-dependent responses among family members. We further analyzed the expression patterns of the *SiSABATH* family across different tissues and under different stress conditions, and found that *SiSABATH9* showed clear responses in multiple tissues and consistent cold stress response patterns among different materials, *SiSABATH9* was selected for further functional evaluation. Furthermore, heterologous expression of *SiSABATH9* in yeast strain BY4741 significantly enhanced tolerance to cold stress.

Conclusions: These findings provide a comprehensive framework of *SABATH* gene structure, classification, evolution, and abiotic stress response in sesame. Furthermore, we identify *SiSABATH9* as a promising cold-responsive candidate gene.

Keywords: SABATH gene family; sesame (*Sesamum indicum* L.); low-temperature stress; methyltransferase; *SiSABATH9*

Background

Plant hormones are widely involved in the regulation of plant growth and development, stress responses and metabolism. The SABATH family comprises plant-specific S-adenosyl-L-methionine (SAM)-dependent methyltransferases that transfer methyl groups to diverse low-molecular-weight substrates, such as salicylic acid (SA), jasmonic acid (JA), indole-3-acetic acid (IAA), and gibberellins (GAs) [1–3]. Structural studies have shown that variation in active-site architecture contributes to substrate recognition within the family [4], while biochemical analyses in different plant lineages have revealed distinct activities toward IAA, SA, JA, and related metabolites [5, 6]. In *Populus*, closely related SABATH methyltransferases differ in substrate preference, and a single amino acid substitution can switch substrate specificity between salicylic acid and benzoic acid [7]. Such biochemical

diversification provides a basis for individual SABATH members to participate in various physiological processes.

Members of the SABATH family regulate plant growth, development, hormone homeostasis, and stress responses through the methylation of signaling molecules. For example, salicylic acid methyltransferases convert salicylic acid (SA) to methyl salicylate (MeSA), which participates in plant defense and systemic acquired resistance in *Clarkia breweri*, *Arabidopsis thaliana*, and *Nicotiana tabacum* [8–10]. Jasmonic acid carboxyl methyltransferases produce methyl jasmonate (MeJA), contributing to jasmonate-regulated responses in *Arabidopsis thaliana* and *Populus trichocarpa* [11, 12]. In addition todefense, *AtIAMT1*-mediated auxin methylation influences leaf development, whereas *AtGAMT1* and *AtGAMT2* regulate gibberellin homeostasis and plant growth [13, 14]. Recent studies have expanded the known substrate range of SABATH enzymes to include carlactonoic acid, a strigolactone-related metabolite involved in shoot branching, and other specialized metabolites [15, 16]. Moreover, *GmSAMT1* enhances *Glycine max* resistance to soybean cyst nematodes [17], while recent studies have identified stress-responsive SABATH genes in cucumber and soybean [18, 19]. These findings highlight the diverse roles of SABATH-mediated methylation in plant development and environmental stress adaptation.

Increasing evidence supports the involvement of *SABATH* genes in environmental responses, but the direction and magnitude of these responses are highly member- and stress-dependent. Tomato *SABATH* genes show gene-specific transcriptional responses to cold, drought, and pathogen challenge [20], whereas *Phaseolus vulgaris* SABATH members respond differentially to drought and salinity and can be modulated by melatonin treatment [21]. Comparable heterogeneity has been reported in tea plant, soybean, and cucumber under biotic and abiotic stresses [18, 19, 22]. Among these environmental stresses, low temperature is particularly relevant because several metabolites modified by SABATH enzymes participate in

cold signaling. Plant cold responses involve extensive transcriptional reprogramming and complex hormone crosstalk [23, 24]. Jasmonate positively regulates freezing tolerance through the ICE–CBF pathway, while salicylic acid also contributes to cold-associated signaling and acclimation [25–27]. More direct evidence showed that the SABATH methyltransferase TaSAMT1 converts SA to MeSA and positively regulates freezing tolerance in wheat [28]. These findings provide a biological basis for investigating SABATH-mediated low-temperature responses in other crops.

Sesame (*Sesamum indicum* L.) is an important oilseed crop with high seed oil content and nutritional quality. High-quality reference genomes and expanding transcriptomic resources have facilitated genome-wide analyses of gene families and stress-response pathways in sesame [29–31]. Several stress-related regulatory gene families, including *bZIP*, *NAC*, *HD-Zip*, *SRO*, *ERF*, and *Trihelix* families, have been systematically characterized in sesame [32–37]. Sesame is sensitive to low temperature during early growth, and different genotypes exhibit considerable variation in sensitivity to cold stress [38]. Recent integrative analyses further indicate that sesame chilling responses involve coordinated transcriptional, metabolic, and sugar-transport changes [39]. However, despite these advances, the *SABATH* gene family has not been systematically characterized in sesame, and the involvement of individual *SiSABATH* members in low-temperature responses remains unclear.

In this study, we systematically identified and characterized *SABATH* family members in sesame by examining their physicochemical properties, chromosomal distribution, collinearity, phylogenetic relationships, conserved motifs, domain architecture, coding-sequence characteristics, promoter cis-acting elements, and tissue-expression patterns. Cold-responsive expression profiles were further evaluated in two cold-tolerant and two cold-sensitive sesame varieties. Based on its consistent transcriptional response across all four genetic backgrounds, *SiSABATH9* was prioritized for functional analysis and evaluated in a

heterologous yeast system under low-temperature stress. This study establishes a genomic and expression framework for the sesame *SABATH* family and identifies *SiSABATH9* as a promising cold-responsive candidate.

Methods

Identification and physicochemical characterization of *SiSABATH* family members

The genome sequence, protein sequences, and corresponding annotation files of sesame (*Sesamum indicum* L.) cultivar Zhongzhi No. 13 were obtained from the improved chromosome-level reference genome [30]. SABATH family members were identified using complementary BLASTP and HMM searches. Characterized *Arabidopsis thaliana* SABATH proteins were used as queries for BLASTP searches against the sesame protein dataset in TBtools-II, with an E-value cutoff of 1×10^{-5} and a maximum of 20 hits retained per query [40, 41]. In parallel, the Hidden Markov model profile of the Methyltransf_7 domain (PF03492) was obtained from Pfam and searched against the sesame protein dataset using the Simple HMM Search function in TBtools-II with an E-value cutoff of 1×10^{-5} [41, 42]. Candidate proteins obtained from the two searches were merged, and redundant sequences were removed. Conserved domains were further verified using NCBI CD-Search with an E-value threshold of 0.01 [43], and proteins with significant matches to the Methyltransf_7 domain were retained as putative *SiSABATH* family members. Protein length, molecular weight, theoretical isoelectric point (pI), instability index, aliphatic index, and grand average of hydropathicity (GRAVY) were calculated using ExPASy ProtParam [44]. Subcellular localization was predicted using WoLF PSORT [45]. The three-dimensional structures of proteins were predicted using the SWISS-MODEL web server.

Chromosomal distribution and collinearity analysis of *SiSABATH* genes

Chromosomal coordinates of *SiSABATH* genes were obtained from the sesame genome annotation and mapped onto the 13 chromosomes using TBtools-II [41]. Gene density along

each chromosome was calculated from the genome annotation and visualized together with the chromosomal positions of *SiSABATH* genes. Genome-wide collinearity analysis was performed using the One Step MCScanX module implemented in TBtools-II based on the sesame genome annotation and protein sequence files [41, 46]. Collinear *SiSABATH* gene pairs located within genome-wide syntenic blocks were considered to be associated with segmental duplication events. The genome assembly and corresponding gene annotation files of *Arabidopsis thaliana*, *Solanum lycopersicum*, and *Vitis vinifera* were downloaded from The Arabidopsis Information Resource (TAIR; https://www.arabidopsis.org/), the Sol Genomics Network (SGN; https://solgenomics.net/organism/solanum_lycopersicum/genome), and Grapedia (https://grapedia.org/genomes/), respectively. Candidate orthologous relationships were identified based on the genome-wide MCScanX results generated by TBtools, and SABATH genes located within conserved syntenic blocks were extracted and visualized.

Phylogenetic, conserved motif, domain, and coding-sequence analyses

Amino acid sequences of 31 SiSABATH proteins, 24 *Arabidopsis thaliana* SABATH proteins, 21 *Oryza sativa* SABATH proteins, and 28 *Glycine max* SABATH proteins were aligned using MUSCLE implemented in MEGA 11 [47, 48]. A neighbor-joining phylogenetic tree was constructed using the Poisson substitution model, uniform substitution rates among sites, and pairwise deletion of gaps and missing data. The resulting tree was visualized and annotated using iTOL [49]. Conserved motifs within the 31 SiSABATH proteins were identified using the MEME Suite, with the maximum number of motifs set to 10 [50]. Positions of the Methyltransf_7 domain were obtained from the conserved-domain analysis described above, and coding-sequence information was extracted from the sesame genome annotation. Phylogenetic relationships, conserved motifs, domain distributions, and coding-sequence characteristics were integrated and visualized using TBtools-II [41].

Promoter cis-acting element analysis

The 2,000-bp genomic sequence upstream of the translation start site of each *SiSABATH* gene was extracted from the sesame reference genome using TBtools-II and defined as the putative promoter region [41]. Cis-acting regulatory elements within these promoter sequences were predicted using PlantCARE [51]. Predicted elements were classified according to their annotated functions, with emphasis on elements associated with phytohormone responses, abiotic-stress responses, and plant growth and development. Their distribution and abundance among *SiSABATH* promoters were subsequently summarized and visualized using TBtools-II.

Expression analysis of *SiSABATH* genes

Expression profiles of *SiSABATH* genes across six sesame tissues, including root, stem, leaf, flower, capsule, and seed, were obtained from previously published RNA-seq data [31]. Transcript abundance was expressed as transcripts per million (TPM), and $\log_2$(TPM + 1)-transformed values were used to visualize tissue-expression patterns. Genes with TPM > 1 were considered expressed, and the distribution and intersections of expressed *SiSABATH* genes among the six tissues were summarized using an UpSet plot. Cold-responsive expression patterns were further analyzed using previously generated expression data from four sesame varieties with contrasting cold tolerance, including two cold-tolerant varieties (A and B) and two cold-sensitive varieties (C and D). Plants maintained at 28 °C served as controls, whereas cold treatment was imposed at 14 °C. Samples were collected after 1, 2, 3, and 4 d of treatment. For each variety and sampling time, transcriptional responses were expressed as $\log_2$ fold changes ($\log_2$FC) relative to the corresponding 28 °C control, with positive and negative values indicating upregulation and downregulation, respectively. Expression-response profiles were visualized using TBtools-II [41], and genes showing consistent responses across the four varieties were prioritized for further functional evaluation.

Functional analysis of *SiSABATH9* in yeast under low-temperature stress

The coding sequence of *SiSABATH9* was cloned into the pYES2-NTB expression vector to generate pYES2-NTB-SiSABATH9. The recombinant vector and the empty pYES2-NTB vector were separately introduced into an environment-sensitive *Saccharomyces cerevisiae* mutant BY4741 using the lithium acetate/polyethylene glycol transformation method and transformants were selected on synthetic dropout medium lacking uracil (SD-Ura) for 3-5 days. The correct positive clones of the experiment group pYES2-NTB-SiSABATH9 and the negative control pYES2-NTB were picked and inoculated into liquid selection medium, after 48h of induction, the bacterial solution was cultured to about an OD600 of 1.5. The initial concentration of the bacterial suspension was uniformly adjusted to OD600 = 0.6，and then serially diluted 10-fold and 100-fold for the subsequent treatment. Cell suspensions described above were exposed to 4, −24, or −28 °C for 24, 48, 72 and 96 h respectively, and spotted onto SG-Ura plates. Photos were taken after the plates were incubated at 30 °C for 3-4-5 days.

Results

Identification and physicochemical characteristics of *SiSABATH* family members

Structural and biochemical studies have shown that SABATH enzymes share a conserved fold while differing in features involved in substrate recognition [4, 7]. To establish the sesame family repertoire and characterize its molecular diversity, we identified candidate members and examined their physicochemical properties, sequence conservation, predicted localization, and structural features. A total of 31 putative SABATH family members were identified in sesame and designated *SiSABATH1–SiSABATH31* according to their chromosomal positions (Table S1). The predicted proteins ranged from 82 to 406 amino acids in length, with molecular weights ranging from 9.36 to 45.76 kDa. Their theoretical isoelectric points ranged from 4.91 to 9.21, instability indices from 33.15 to 59.47, aliphatic indices from 70.67 to 96.05, and

GRAVY values from −0.404 to 0.177. With the exception of SiSABATH5, all SiSABATH proteins had negative GRAVY values, indicating that most members were hydrophilic. The coding-sequence lengths ranged from 246 to 1,218 bp, whereas genomic lengths ranged from 249 to 9,953 bp. All SiSABATH proteins were annotated with the characteristic Methyltransf_7 domain, although SiSABATH13 was markedly shorter than the other family members and showed only partial domain coverage. Predicted subcellular localization indicated that SiSABATH proteins were mainly distributed in the cytoplasm and nucleus (Table S2), with nine proteins predicted in each compartment, followed by the chloroplast (six), cytoskeleton (four), and mitochondrion (three). Multiple sequence alignment revealed substantial amino acid sequence conservation among the 31 SiSABATH proteins, particularly in several regions of the central and C-terminal portions (Fig. S1). In contrast, the N-terminal regions and certain internal segments exhibited greater sequence variability, including amino acid insertions, deletions, and differences in sequence length. Although the overall distribution of conserved regions was similar among family members, variations in amino acid composition were observed in specific regions. The predicted three-dimensional structures of the 31 SiSABATH proteins exhibited variations in overall conformation, compactness, and the arrangement of structural regions (Fig. S2). Most proteins displayed compact, globular structures, whereas some members showed extended terminal regions or more pronounced structural differences.

Chromosomal distribution and collinearity analysis

Gene duplication has contributed to SABATH family expansion in tea plant, *Arabidopsis*, and rice [22, 52]. We therefore examined chromosomal distribution and intra- and interspecific collinearity to assess duplication patterns and conserved genomic relationships among *SiSABATH* genes. The 31 *SiSABATH* genes were unevenly distributed across nine of the 13 sesame chromosomes (Fig. 1A). Chromosome 2 contained the largest number of *SiSABATH*

genes, with 13 members, followed by chromosome 11 with six. Chromosomes 1 and 3 each contained three members, chromosome 12 contained two, and chromosomes 6, 7, 10, and 13 each contained one. No *SiSABATH* genes were detected on chromosomes 4, 5, 8, or 9. Genome-wide collinearity analysis identified three *SiSABATH* collinear gene pairs: *SiSABATH1–SiSABATH14*, *SiSABATH20–SiSABATH21*, and *SiSABATH21–SiSABATH31* (Fig. 1B). All three pairs were located within genome-wide collinear blocks, suggesting that segmental duplication contributed to the evolution of at least part of the *SiSABATH* gene family. Comparative synteny analysis revealed collinear relationships between *Sesamum indicum* SABATH genes and their counterparts in *Arabidopsis thaliana*, *Solanum lycopersicum*, and *Vitis vinifera* (Fig. S3). A total of 16, 8, and 10 syntenic gene pairs were identified between *Sesamum indicum* and *Arabidopsis thaliana*, *Solanum lycopersicum*, and *Vitis vinifera*, respectively (Table S3).

Phylogenetic relationships and conserved characteristics

Phylogenetic and sequence comparisons have provided a framework for investigating SABATH evolution and proposing functional relationships among family members [6, 53]. To define the relationships and conserved features of SiSABATH proteins, we jointly examined their phylogeny, motif composition, domain organization, and coding-sequence characteristics. Phylogenetic analysis of 104 SABATH proteins from sesame, *Arabidopsis*, rice, and soybean classified the family into six major groups (Groups I–VI) (Fig. 2). The 31 SiSABATH proteins were distributed among four groups. Group I contained the largest number of sesame members, comprising 19 SiSABATH proteins. Groups III and IV each contained three SiSABATH proteins, whereas six members were assigned to Group VI. No sesame SABATH proteins were present in Groups II or V. SiSABATH9 was assigned to Group I. Ten conserved motifs were identified among the 31 SiSABATH proteins (Fig. 3A). Motif 1, Motif 3, and Motif 6 were the longest motifs (50 aa each), whereas Motif 7 and Motif 10 were

the shortest (15 aa each). Regarding motif occurrence, Motif 4 was detected at the largest number of sites (28), while Motif 8 was detected at the fewest sites (13). Motif 1, Motif 2, Motif 3, and Motif 7 were each detected at 26 sites (Fig. S4). Phylogenetically related proteins generally showed similar motif compositions and arrangements, although variation was evident among groups. SiSABATH13 contained only Motif 5 and was clearly distinct from most other family members. The Methyltransf_7 domain was detected across the family, although domain coverage varied among proteins, with SiSABATH13 showing only partial coverage (Fig. 3B). Coding-sequence lengths also varied considerably among SiSABATH genes (Fig. 3C), further illustrating structural variation within the family.

Cis-acting elements in *SiSABATH* promoters

Predicted hormone- and stress-associated cis-elements have been reported in SABATH promoters of cucumber and *Neolamarckia cadamba* [18, 54]. To identify candidate regulatory inputs for the sesame family, we surveyed *SiSABATH* promoters for elements associated with environmental responses, hormone signaling, and development. A diverse range of cis-acting regulatory elements was identified in the promoter regions of the 31 *SiSABATH* genes (Fig. 4). These elements were grouped into three major functional categories: abiotic and biotic stress responses, phytohormone responses, and plant growth and development. Stress-related elements included MYB-, MYC-, W-box-, and LTR-related motifs; hormone-responsive elements included ABRE and MeJA-responsive motifs; and growth- and development-related elements included light-responsive elements such as Box 4 and G-box. The composition and abundance of cis-acting elements differed markedly among family members. Low-temperature-responsive LTR elements were present in the promoters of 12 *SiSABATH* genes. *SiSABATH28*, *SiSABATH19*, *SiSABATH1*, and *SiSABATH3* contained relatively high total numbers of predicted cis-acting elements compared with other family members, revealing substantial variation in promoter regulatory architecture across the family.

Tissue expression patterns of *SiSABATH* genes

Functional studies have linked SABATH-mediated hormone methylation to leaf development and gibberellin homeostasis [13, 14]. We therefore compared *SiSABATH* transcript abundance across vegetative and reproductive tissues to distinguish broadly expressed members from those with tissue-preferential expression and identify candidates for developmental studies. Tissue-expression analysis revealed substantial spatial variation among the 31 *SiSABATH* genes across capsule, seed, flower, leaf, stem, and root tissues (Fig. 5A). Several genes were expressed across multiple tissues, whereas others showed restricted or tissue-preferential expression patterns. Differences were also evident among members belonging to the same phylogenetic group. Using TPM > 1 as the threshold for detectable expression, seed, flower, and root each contained 12 expressed *SiSABATH* genes, whereas leaf, capsule, and stem each contained nine (Fig. 5B). Three genes were expressed in all six tissues, while three were detected exclusively in flower. Two genes were exclusively expressed in seed and two exclusively in root. Two-gene intersections were also observed for the capsule–seed, seed–root, and leaf–stem–root combinations, as well as for genes expressed in all tissues except leaf. Several additional tissue combinations contained a single *SiSABATH* gene. Together, these patterns demonstrate pronounced spatial heterogeneity among *SiSABATH* family members.

Expression patterns under abiotic stress

SABATH genes exhibit differential transcriptional responses to drought and salinity in cucumber and common bean [18, 21]. To identify stress-responsive members and assess response specificity in sesame, we compared *SiSABATH* expression profiles under drought, waterlogging, salt, and alkali stresses. The *SiSABATH* genes exhibited distinct expression patterns under the four abiotic stresses (Fig.6). Salt stress was mainly associated with decreased expression, whereas drought induced both increases and decreases among different

297 members. Expression changes under waterlogging and alkali stress were generally more
298 moderate. Several genes showed contrasting responses across stress conditions, reflecting
299 variation in the transcriptional responses of the SiSABATH family. To further identify
300 cold-responsive candidates with reproducible responses across genetic backgrounds, we
301 compared expression profiles over time in the four varieties with contrasting cold tolerance.
302 Cold treatment induced distinct transcriptional responses among the 31 *SiSABATH* genes, with
303 both the direction and magnitude of expression changes varying among genotypes and
304 treatment durations (Fig. 7). Several Group I members, including *SiSABATH1*, *SiSABATH2*,
305 *SiSABATH5*, *SiSABATH9*, *SiSABATH14*, *SiSABATH18*, and *SiSABATH19*, showed relatively
306 pronounced changes under particular treatment conditions, whereas many members of Groups
307 III, IV, and VI exhibited weaker or more condition-dependent responses. Among the family
308 members, *SiSABATH9* showed the most reproducible early response. At 2 d of cold treatment,
309 *SiSABATH9* was consistently upregulated in both cold-tolerant varieties (A and B) and
310 cold-sensitive varieties (C and D), whereas its responses at 1, 3, and 4 d were weaker and more
311 genotype dependent. Other *SiSABATH* genes generally showed greater genotype dependence,
312 and some exhibited opposite response directions at different treatment durations. The
313 consistent 2-d induction of *SiSABATH9* across the four genetic backgrounds therefore provided
314 the basis for its prioritization for subsequent functional analysis.

315 **Functional analysis of *SiSABATH9* in cold stress**

316 Experimental studies have linked jasmonate signaling and SABATH-mediated salicylic
317 acid methylation to freezing tolerance [25, 28]. To test whether the cold-responsive candidate
318 *SiSABATH9* can promote recovery after low-temperature exposure, we expressed
319 *SiSABATH9* in yeast strain BY4741 and compared it with the empty-vector control. Cell
320 suspensions carrying pYES2-NTB-*SiSABATH9* or the empty pYES2-NTB vector were
321 exposed to 4, −24, or −28 °C for 24, 48, 72, or 96 h before being spotted onto SG-Ura plates.

SiSABATH9-expressing yeast and the empty-vector control showed comparable growth recovery after 4 °C treatment, whereas treatment-dependent differences were observed after freezing at −24 and −28 °C (Fig. 8). After 48 h at −24 °C, *SiSABATH9*-expressing yeast retained detectable growth, whereas the empty-vector control was strongly inhibited. A more pronounced difference was observed under −28 °C treatment. *SiSABATH9*-expressing cells showed markedly better growth recovery than the empty-vector control after 24, 48, and 72 h of exposure, whereas growth of the control strain was severely restricted. After 96 h at −24 or −28 °C, neither strain showed obvious recovery. These results indicate that *SiSABATH9* expression improved post-freezing growth recovery in yeast.

Discussion

The *SABATH* gene family shows considerable variation in family size and evolutionary organization among plant species. In sesame, 31 *SiSABATH* members were identified, a family size similar to the 32 members reported in tea plant and 28 in soybean, but larger than the 21 members identified in rice and 13 in cucumber [18, 19, 22, 52]. Gene duplication is an important force in plant gene-family evolution. Tandem duplication has contributed strongly to SABATH family expansion in tea plant, whereas both tandem and segmental duplication have contributed to the family in *Arabidopsis* and rice [22, 52]. In sesame, three collinear *SiSABATH* gene pairs were identified, indicating that segmental duplication contributed to the evolution of at least part of the family. Phylogenetically, SiSABATH proteins were restricted to Groups I, III, IV, and VI, with 19 of the 31 members assigned to Group I. Closely related SiSABATH proteins generally shared similar motif and domain architectures, whereas several members showed clear structural divergence. Similar family-level analyses in silver birch have suggested distinct putative substrate preferences among phylogenetically related SABATH/MES members [53]. However, such predictions require biochemical validation because substrate recognition can depend on relatively subtle structural differences, as

demonstrated by structural and functional studies of SABATH enzymes [4, 7]. Thus, the evolutionary and structural patterns observed in sesame are consistent with a family that combines conserved catalytic architecture with member-specific functional diversification.

This structural diversity was accompanied by pronounced regulatory and spatial differentiation. In sesame, some *SiSABATH* genes were broadly expressed across multiple tissues, whereas others showed restricted expression; notably, three genes were expressed across all six examined tissues and three were detected exclusively in flowers. Comparable tissue-preferential expression has been reported in tea plant, soybean, and cucumber, where individual *SABATH* members differ markedly among vegetative and reproductive tissues [18, 19, 22]. Regulatory diversity is also evident in other species: NcSABATH promoters in *Neolamarckia cadamba* contain numerous light-, hormone-, and stress-responsive elements, and individual family members show distinct tissue-expression profiles [54]. Consistent with these observations, *SiSABATH* promoters contained abundant hormone- and stress-responsive cis-acting elements, including LTR elements in 12 genes, and differed substantially in overall cis-element composition. Together, the promoter and tissue-expression data indicate that individual *SiSABATH* members are likely subject to distinct regulatory programs and may respond differently to developmental and environmental cues.

These regulatory differences were further reflected in stress-responsive expression. In *Camellia sinensis*, *SABATH* genes generally responded more strongly to MeJA treatment and herbivore feeding than to cold acclimation [22]. Tomato SABATH members show gene-specific responses to cold, drought, and pathogen challenge [20], whereas *Phaseolus vulgaris SABATH* genes respond differentially to drought and salinity [21]. Cucumber SABATH *genes* also display gene-specific responses to drought and salt stress, and soybean SABATH members respond heterogeneously to salt and metal stresses [18, 19]. A similarly diverse pattern was observed in sesame, where both the direction and magnitude of *SiSABATH*

expression changes varied with treatment duration and genetic background. Among these genes, *SiSABATH9* was notable for its reproducible response across all four varieties, being consistently upregulated at 2 d of cold treatment in both cold-tolerant and cold-sensitive genotypes, whereas its responses at other sampling times were weaker and more genotype dependent. This cross-genotype consistency, rather than the magnitude of expression change alone, provided the primary basis for prioritizing *SiSABATH9* for functional analysis.

Based on this consistent cold-responsive pattern, *SiSABATH9* was further evaluated in a heterologous yeast system. *SiSABATH9*-expressing yeast showed improved growth recovery under severe low-temperature treatments compared with the empty-vector control, providing additional functional support for an association between *SiSABATH9* and low-temperature responses. This interpretation is biologically plausible because several known SABATH substrates participate in cold signaling. Jasmonate promotes freezing tolerance through regulation of the ICE–CBF pathway, while salicylic acid is also involved in plant responses to low temperature [25–27]. More direct evidence linking a SABATH methyltransferase to freezing tolerance comes from wheat TaSAMT1, which catalyzes the conversion of salicylic acid to methyl salicylate and positively regulates freezing tolerance [28]. Nevertheless, the functional similarity between TaSAMT1 and SiSABATH9 does not establish a shared biochemical mechanism. SABATH proteins can act on chemically diverse substrates; for example, closely related *Populus* proteins exhibit different preferences for IAA, SA/benzoic acid, and farnesoic acid, while an Arabidopsis SABATH methyltransferase catalyzes methylation of carlactonoic acid [7, 15]. Therefore, the current expression and heterologous functional evidence support *SiSABATH9* as a promising cold-responsive candidate, while its biochemical substrate and precise physiological mechanism in sesame remain unresolved.

Conclusions

In conclusion, this study identified 31 *SiSABATH* genes, and these members exhibited substantial diversity in phylogenetic distribution, structural organization, promoter composition, and tissue-expression patterns. The predicted hormone- and stress-associated motifs and the heterogeneous expression profiles under drought, waterlogging, salt, and alkali stresses provide candidate genes and regulatory sites for further investigation. Under low-temperature treatment, expression responses varied with treatment duration and genotype, with *SiSABATH9* consistently upregulated at 2 d of treatment across all four sesame varieties. Its heterologous expression improved yeast growth recovery after freezing at −24 °C and −28 °C. Taken together, these results identify *SiSABATH9* as a promising cold-responsive candidate gene and provide a basis for further understanding the role of SABATH methyltransferases in sesame responses to low-temperature stress.

References

1. D'Auria JC, Chen F, Pichersky E. The SABATH family of MTs in *Arabidopsis thaliana* and other plant species. *Recent Adv Phytochem.* 2003;37:253–283.

2. Qu L, Li S, Xing S. Methylation of phytohormones by the SABATH methyltransferases. *Chin Sci Bull.* 2010;55:2211–2218.

3. Wang W, Guo H, Bowman JL, Chen F. Plant SABATH methyltransferases: diverse functions, unusual reaction mechanisms and complex evolution. *Crit Rev Plant Sci.* 2024;43:291–312.

4. Zubieta C, Ross JR, Koscheski P, Yang Y, Pichersky E, Noel JP. Structural basis for substrate recognition in the salicylic acid carboxyl methyltransferase family. *Plant Cell.* 2003;15:1704–1716.

5. Chaiprasongsuk M, Zhang C, Qian P, Chen X, Li G, Trigiano RN, et al. Biochemical characterization in Norway spruce (*Picea abies*) of SABATH methyltransferases that methylate phytohormones. *Phytochemistry.* 2018;149:146–154.

6. Zhao N, Ferrer JL, Ross J, Guan J, Yang Y, Pichersky E, et al. Structural, biochemical, and phylogenetic analyses suggest that indole-3-acetic acid methyltransferase is an evolutionarily ancient member of the SABATH family. *Plant Physiol.* 2008;146:455–467.

7. Han XM, Yang Q, Liu YJ, Yang ZL, Wang XR, Zeng QY, et al. Evolution and function of the *Populus* SABATH family reveal that a single amino acid change results in a substrate switch. *Plant Cell Physiol.* 2018;59:392–403.

8. Ross JR, Nam KH, D'Auria JC, Pichersky E. S-Adenosyl-L-methionine:salicylic acid carboxyl methyltransferase, an enzyme involved in floral scent production and plant defense, represents a new class of plant methyltransferases. *Arch Biochem Biophys.* 1999;367:9–16.

9. Chen F, D'Auria JC, Tholl D, Ross JR, Gershenzon J, Noel JP, et al. An *Arabidopsis thaliana* gene for methylsalicylate biosynthesis, identified by a biochemical genomics approach, has a role in defense. *Plant J.* 2003;36:577–588.

10. Park SW, Kaimoyo E, Kumar D, Mosher S, Klessig DF. Methyl salicylate is a critical mobile signal for plant systemic acquired resistance. *Science.* 2007;318:113–116.

11. Seo HS, Song JT, Cheong JJ, Lee YH, Lee YW, Hwang I, et al. Jasmonic acid carboxyl methyltransferase: a key enzyme for jasmonate-regulated plant responses. *Proc Natl Acad Sci U S A.* 2001;98:4788–4793.

12. Zhao N, Yao J, Chaiprasongsuk M, Li G, Guan J, Tschaplinski TJ, et al. Molecular and biochemical characterization of the jasmonic acid methyltransferase gene from black cottonwood (*Populus trichocarpa*). *Phytochemistry.* 2013;94:74–81.

13. Qin G, Gu H, Zhao Y, Ma Z, Shi G, Yang Y, et al. An indole-3-acetic acid carboxyl methyltransferase regulates *Arabidopsis* leaf development. *Plant Cell.* 2005;17:2693–2704.

14. Varbanova M, Yamaguchi S, Yang Y, McKelvey K, Hanada A, Borochov R, et al. Methylation of gibberellins by *Arabidopsis* GAMT1 and GAMT2. *Plant Cell.* 2007;19:32–45.

15. Mashiguchi K, Seto Y, Onozuka Y, Suzuki S, Takemoto K, Wang Y, et al. A carlactonoic acid methyltransferase that contributes to the inhibition of shoot branching in *Arabidopsis*. *Proc Natl Acad Sci U S A.* 2022;119:e2111565119.

16. Zhuge XL, Du X, Xiu ZJ, He CC, Wang YM, Yang HL, et al. Discovery of specific catalytic activity toward IAA/FA by LaSABATHs based on genome-wide phylogenetic and enzymatic analysis of SABATH gene family from *Larix kaempferi*. *Int J Biol Macromol.* 2023;225:1562–1574.

17. Lin J, Mazarei M, Zhao N, Hatcher CN, Wuddineh WA, Rudis M, et al. Transgenic soybean overexpressing *GmSAMT1* exhibits resistance to multiple-HG types of soybean cyst nematode *Heterodera glycines*. *Plant Biotechnol J.* 2016;14:2100–2109.

18. Zhang X, Li S, Zhou Y, Chen M, Jiang L, Fu W. Characterization and expression analysis of the SABATH gene family under abiotic stresses in cucumber (*Cucumis sativus* L.). *Plants.* 2025;14:1748.

19. Wen K, Zhong W, Feng L, Han T, Suo H, Ren H, et al. Genome-wide identification of SABATH gene family in soybean relate to salt, aluminum, chromium toxicity. *Sci Rep.* 2025;15:14030.

20. Wei X, Tao K, Zhang J, Lu S, Chen S, Liao J. Identification of SABATH family members in *Solanum lycopersicum* and their expression patterns under abiotic/biotic stresses. *Plant Mol Biol Rep.* 2021;39:403–418.

21. Aygören AS, Güneş E, Muslu S, Kasapoğlu AG, Yiğider E, Aydın M, et al. Genome-wide analysis and characterization of SABATH gene family in *Phaseolus vulgaris* genotypes subject to melatonin under drought and salinity stresses. *Plant Mol Biol Rep.* 2023;41:242–259.

22. Guo Y, Qiao D, Yang C, Chen J, Li Y, Liang S, et al. Genome-wide identification and expression analysis of SABATH methyltransferases in tea plant (*Camellia sinensis*): insights into their roles in plant defense responses. *Plant Signal Behav.* 2020;15:1804684.

23. Eremina M, Rozhon W, Poppenberger B. Hormonal control of cold stress responses in plants. *Cell Mol Life Sci.* 2016;73:797–810.

24. Kidokoro S, Shinozaki K, Yamaguchi-Shinozaki K. Transcriptional regulatory network of plant cold-stress responses. *Trends Plant Sci.* 2022;27:922–935.

25. Hu Y, Jiang L, Wang F, Yu D. Jasmonate regulates the inducer of CBF expression–C-repeat binding factor/DRE binding factor1 cascade and freezing tolerance in *Arabidopsis*. *Plant Cell.* 2013;25:2907–2924.

26. Hu Y, Jiang Y, Han X, Wang H, Pan J, Yu D. Jasmonate regulates leaf senescence and tolerance to cold stress: crosstalk with other phytohormones. *J Exp Bot.* 2017;68:1361–1369.

27. Miura K, Tada Y. Regulation of water, salinity, and cold stress responses by salicylic acid. *Front Plant Sci.* 2014;5:4.

28. Chu W, Chang S, Lin J, Zhang C, Li J, Liu X, et al. Methyltransferase *TaSAMT1* mediates wheat freezing tolerance by integrating brassinosteroid and salicylic acid signaling. *Plant Cell.* 2024;36:2607–2628.

29. Avashthi H, Angadi UB, Chauhan D, Kumar A, Mishra DC, Rangan P, et al. Sesame Genomic Web Resource (SesameGWR): a well-annotated data resource for

493 transcriptomic signatures of abiotic and biotic stress responses in sesame (*Sesamum*
494 *indicum* L.). *Brief Funct Genomics.* 2024;23:828–842.
495 30. Song S, Dossou SSK, Meng M, Sheng C, Li H, Zhou R, et al. Five improved
496 sesame reference genomes and genome resequencing unveil the contribution of structural
497 variants to genetic diversity and yield-related traits variation. *Plant Biotechnol J.*
498 2023;21:1722–1724.
499 31. Wang L, Yu S, Tong C, Zhao Y, Liu Y, Song C, et al. Genome sequencing of
500 the high oil crop sesame provides insight into oil biosynthesis. *Genome Biol.*
501 2014;15:R39.
502 32. Liu A, Wei M, Zhou Y, Li D, Zhou R, Zhang Y, et al. Comprehensive analysis
503 of SRO gene family in *Sesamum indicum* (L.) reveals its association with abiotic stress
504 responses. *Int J Mol Sci.* 2021;22:13048.
505 33. Su R, Dossou SSK, Dossa K, Zhou R, Liu A, Zhong Y, et al. Genome-wide
506 characterization and identification of candidate ERF genes involved in various abiotic
507 stress responses in sesame (*Sesamum indicum* L.). *BMC Plant Biol.* 2022;22:256.
508 34. Wang Y, Zhang Y, Zhou R, Dossa K, Yu J, Li D, et al. Identification and
509 characterization of the bZIP transcription factor family and its expression in response to
510 abiotic stresses in sesame. *PLoS One.* 2018;13:e0200850.
511 35. Wei M, Liu A, Zhang Y, Zhou Y, Li D, Dossa K, et al. Genome-wide
512 characterization and expression analysis of the HD-Zip gene family in response to
513 drought and salinity stresses in sesame. *BMC Genomics.* 2019;20:748.
514 36. Zhang Y, Li D, Wang Y, Zhou R, Wang L, Zhang Y, et al. Genome-wide
515 identification and comprehensive analysis of the NAC transcription factor family in
516 *Sesamum indicum*. *PLoS One.* 2018;13:e0199262.

517 37. Zhao Y, Liang J, Wang Z, Yan T, Yan X, Wei W, et al. Genome-wide
518 identification and expression analysis of the trihelix transcription factor family in sesame
519 (*Sesamum indicum* L.) under abiotic stress. *Mol Biol Rep.* 2023;50:8281–8295.
520 38. Abbas AA, Berhe M, Kefale H, Hussien SA, Zhou R, Zhou T, et al.
521 Physiological and biochemical responses to cold stress in sesame (*Sesamum indicum* L.)
522 during the early growth stage. *Plant Soil Environ.* 2025;71:293–307.
523 39. Zeng P, Zhao Y, Liang J, Yan X, Wang Z, Sun J. Genome-wide identification of
524 SWEET gene family and integrative transcriptomic–metabolomic analysis reveal sugar
525 transport-mediated chilling responses in sesame (*Sesamum indicum* L.). *Curr Issues Mol*
526 *Biol.* 2026;48:312.
527 40. Altschul SF, Madden TL, Schäffer AA, Zhang J, Zhang Z, Miller W, et al.
528 Gapped BLAST and PSI-BLAST: a new generation of protein database search programs.
529 *Nucleic Acids Res.* 1997;25:3389–3402.
530 41. Chen C, Wu Y, Li J, Wang X, Zeng Z, Xu J, et al. TBtools-II: a “one for all, all
531 for one” bioinformatics platform for biological big-data mining. *Mol Plant.*
532 2023;16:1733–1742.
533 42. Mistry J, Chuguransky S, Williams L, Qureshi M, Salazar GA, Sonnhammer
534 ELL, et al. Pfam: the protein families database in 2021. *Nucleic Acids Res.*
535 2021;49:D412–D419.
536 43. Marchler-Bauer A, Derbyshire MK, Gonzales NR, Lu S, Chitsaz M, Geer LY, et
537 al. CDD: NCBI’s conserved domain database. *Nucleic Acids Res.* 2015;43:D222–D226.
538 44. Gasteiger E, Hoogland C, Gattiker A, Duvaud S, Wilkins MR, Appel RD, et al.
539 Protein identification and analysis tools on the ExPASy server. In: Walker JM, editor.
540 *The Proteomics Protocols Handbook*. Totowa, NJ: Humana Press; 2005. pp. 571–607.

45. Horton P, Park KJ, Obayashi T, Fujita N, Harada H, Adams-Collier CJ, et al. WoLF PSORT: protein localization predictor. *Nucleic Acids Res.* 2007;35:W585–W587.

46. Wang Y, Tang H, DeBarry JD, Tan X, Li J, Wang X, et al. MCScanX: a toolkit for detection and evolutionary analysis of gene synteny and collinearity. *Nucleic Acids Res.* 2012;40:e49.

47. Edgar RC. MUSCLE: multiple sequence alignment with high accuracy and high throughput. *Nucleic Acids Res.* 2004;32:1792–1797.

48. Tamura K, Stecher G, Kumar S. MEGA11: molecular evolutionary genetics analysis version 11. *Mol Biol Evol.* 2021;38:3022–3027.

49. Letunic I, Bork P. Interactive Tree Of Life (iTOL) v5: an online tool for phylogenetic tree display and annotation. *Nucleic Acids Res.* 2021;49:W293–W296.

50. Bailey TL, Johnson J, Grant CE, Noble WS. The MEME Suite. *Nucleic Acids Res.* 2015;43:W39–W49.

51. Lescot M, Déhais P, Thijs G, Marchal K, Moreau Y, Van de Peer Y, et al. PlantCARE, a database of plant cis-acting regulatory elements and a portal to tools for in silico analysis of promoter sequences. *Nucleic Acids Res.* 2002;30:325–327.

52. Wang B, Li M, Yuan Y, Liu S. Genome-wide comprehensive analysis of the SABATH gene family in *Arabidopsis* and rice. *Evol Bioinform (Online).* 2019;15:1176934319860864.

53. Singewar K, Moschner CR, Hartung E, Fladung M. Genome-wide bioinformatics analysis revealed putative substrate specificities of SABATH and MES family members in silver birch (*Betula pendula*). *Silvae Genet.* 2021;70:57–74.

54. Ren R, Zhang S, Guo T, Long J, Peng C. Genome-wide identification and expression pattern analysis of the SABATH gene family in *Neolamarckia cadamba*. *Forestry Res.* 2023;3:13.

Declarations

Ethics approval and consent to participate

Not applicable.

Consent for publication

Not applicable.

Acknowledgements

Not applicable.

Availability of data and materials

The datasets used and/or analysed during the current study are available from the corresponding author on reasonable request.

Competing interests

The authors declare no competing interests.

Funding

This work was financially supported by the National Natural Science Foundation of China (No. 32401748), National Science and Technology Resource Sharing Service Platform-National Crop Germplasm Resources Center (NCGRC-2026-016), the Hubei Provincial Natural Science Foundation of China (2026AFC0637), the China Agriculture Research System (CARS-14); Central Public-interest Scientific Institution Basal Research Fund (No.1610172026007).

Authors' contributions

LY and YZ conceived and designed the experiments; XQ performed the experiments; XH, YW, LF, LW, HL and JY participated in data collection and analysis; XQ and LY wrote the paper. All authors have read and approved the final manuscript.

589 **Figure legends**

590 **Fig. 1 Chromosomal distribution and collinearity of *SiSABATH* genes in sesame.** (A)
591 Chromosomal distribution of the 31 *SiSABATH* genes. The chromosome heatmap represents
592 local gene density, with colors from blue to red indicating increasing gene density. (B)
593 Genome-wide collinearity map of sesame. Gray links represent genome-wide collinear
594 regions, whereas red links highlight collinear *SiSABATH* gene pairs.

595 **Fig. 2 Phylogenetic relationships of SABATH proteins from *Sesamum indicum*,**
596 ***Arabidopsis thaliana*, *Oryza sativa*, and *Glycine max*.** The tree comprises 31 SiSABATH, 24
597 AtSABATH, 21 OsSABATH, and 28 GmSABATH proteins and is classified into six major
598 groups (I–VI). Red triangles, green asterisks, orange squares, and blue diamonds represent
599 proteins from *S. indicum*, *A. thaliana*, *O. sativa*, and *G. max*, respectively.

600 **Fig. 3 Conserved motif, domain, and coding-sequence characteristics of SiSABATH**
601 **family members.** (A) Distribution of 10 conserved motifs among SiSABATH proteins.
602 Different colors represent distinct motifs. (B) Distribution of the Methyltransf_7 domain. (C)
603 Coding-sequence lengths of *SiSABATH* genes.

604 **Fig. 4 Distribution and abundance of cis-acting regulatory elements in *SiSABATH***
605 **promoters.** Predicted elements are grouped into abiotic and biotic stress responses,
606 phytohormone responses, and plant growth and development. Darker shading indicates higher
607 abundance, and stacked bars show the total number of elements in each functional category for
608 each gene.

609 **Fig. 5 Tissue expression patterns of *SiSABATH* genes in sesame.** (A) Circular heatmap
610 showing expression profiles in capsule, seed, flower, leaf, stem, and root. Expression levels are
611 shown as $\log_2$ (TPM + 1), and the outer ring indicates phylogenetic group. (B) UpSet plot
612 showing the distribution and intersections of expressed *SiSABATH* genes among the six tissues.
613 Genes with TPM > 1 were considered expressed.

Fig. 6 Expression patterns of SiSABATH genes under four abiotic stresses.

Fig. 7 Cold-responsive expression profiles of *SiSABATH* genes in sesame varieties with contrasting cold tolerance. Expression changes are shown for two cold-tolerant varieties (A and B) and two cold-sensitive varieties (C and D) after 1, 2, 3, and 4 d of cold treatment. Bubble color represents signed $\log_2$ fold change ($\log_2$FC), bubble size represents |$\log_2$FC|, background shading indicates phylogenetic group, and annotation bars indicate cold-tolerance class and treatment duration.

Fig. 8 Functional analysis of *SiSABATH9* in yeast under low-temperature stress. Growth recovery of *Saccharomyces cerevisiae* cells expressing *SiSABATH9* or carrying the empty vector after exposure to 4, −24, or −28 °C for 24, 48, 72, or 96 h.

Supplementary Materials:

Fig. S1 Multiple sequence alignment of SiSABATH proteins.

Fig. S2 Predicted three-dimensional structures of the 31 SiSABATH proteins.

Fig. S3 Synteny analysis of SABATH genes between sesame and other representative plant species.

Fig. S4 Sequence logos of the 10 conserved motifs identified in SiSABATH proteins.

Supplementary Table S1 Detailed information of *SiSABATH* genes.

Supplementary Table S2 Sequence Characteristics of *SiSABATH* genes.

Supplementary Table S3 Syntenic gene pairs of SABATH between sesame and three plant species.

(A)

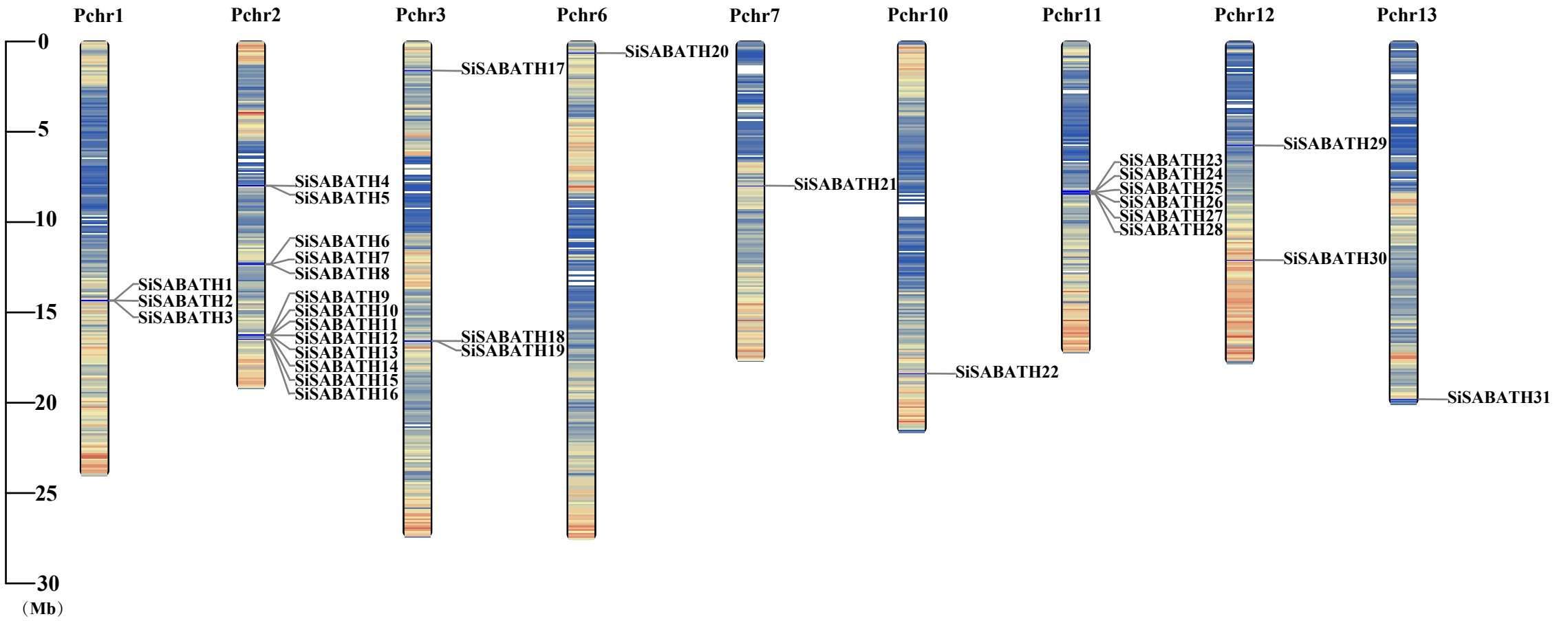
Pchr1
Pchr2
Pchr3
Pchr6
Pchr7
Pchr10
Pchr11
Pchr12
Pchr13
0
5
10
15
20
25
30
(Mb)
SiSABATH1
SiSABATH2
SiSABATH3
SiSABATH4
SiSABATH5
SiSABATH6
SiSABATH7
SiSABATH8
SiSABATH9
SiSABATH10
SiSABATH11
SiSABATH12
SiSABATH13
SiSABATH14
SiSABATH15
SiSABATH16
SiSABATH17
SiSABATH18
SiSABATH19
SiSABATH20
SiSABATH21
SiSABATH22
SiSABATH23
SiSABATH24
SiSABATH25
SiSABATH26
SiSABATH27
SiSABATH28
SiSABATH29
SiSABATH30
SiSABATH31

(B)

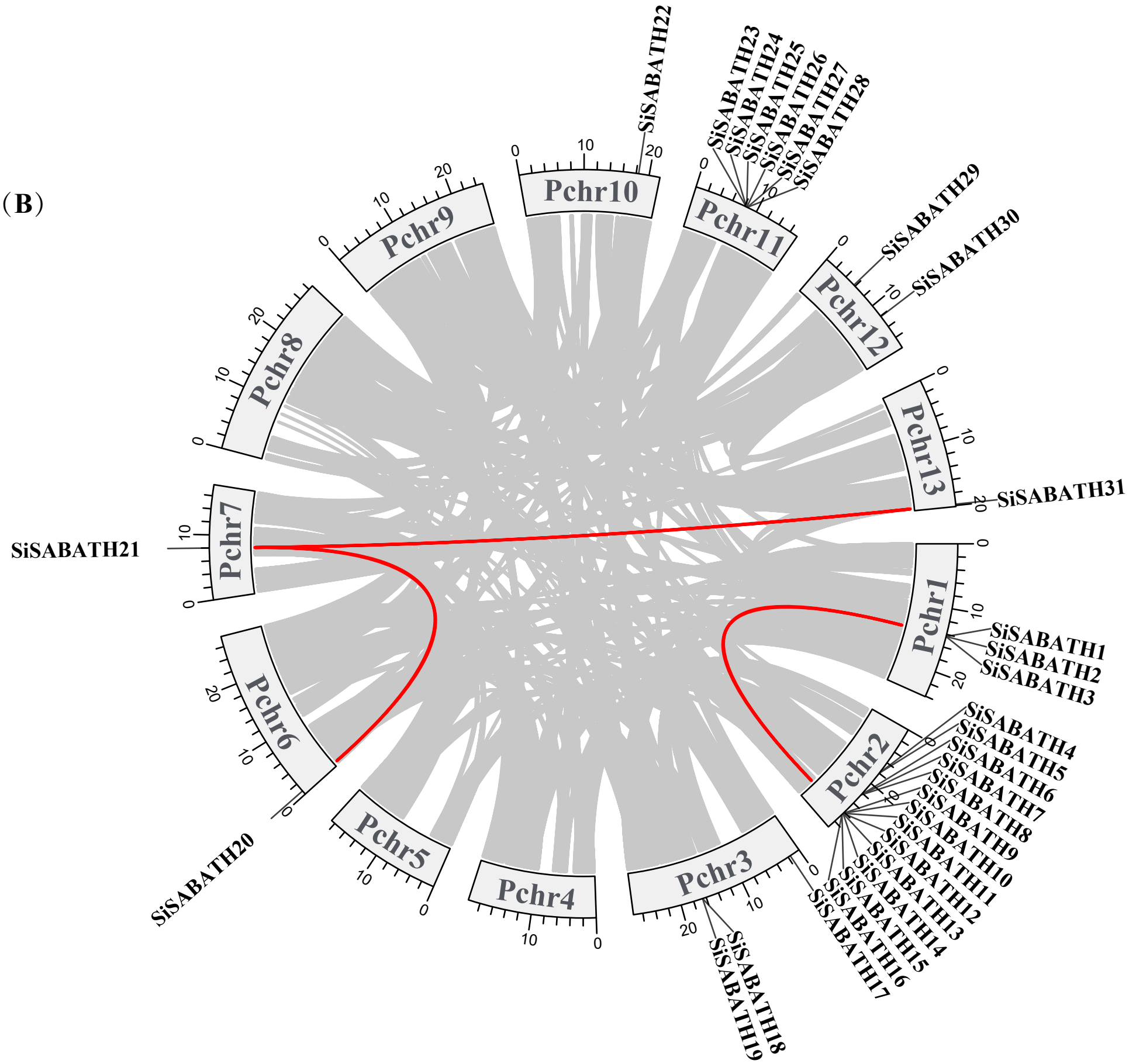
Pchr9
Pchr10
Pchr11
Pchr12
Pchr13
Pchr8
Pchr7
Pchr6
Pchr5
Pchr4
Pchr3
Pchr2
Pchr1
SiSABATH22
SiSABATH23
SiSABATH24
SiSABATH25
SiSABATH26
SiSABATH27
SiSABATH28
SiSABATH29
SiSABATH30
SiSABATH31
SiSABATH21
SiSABATH20
SiSABATH1
SiSABATH2
SiSABATH3
SiSABATH4
SiSABATH5
SiSABATH6
SiSABATH7
SiSABATH8
SiSABATH9
SiSABATH10
SiSABATH11
SiSABATH12
SiSABATH13
SiSABATH14
SiSABATH15
SiSABATH16
SiSABATH17
SiSABATH18
SiSABATH19

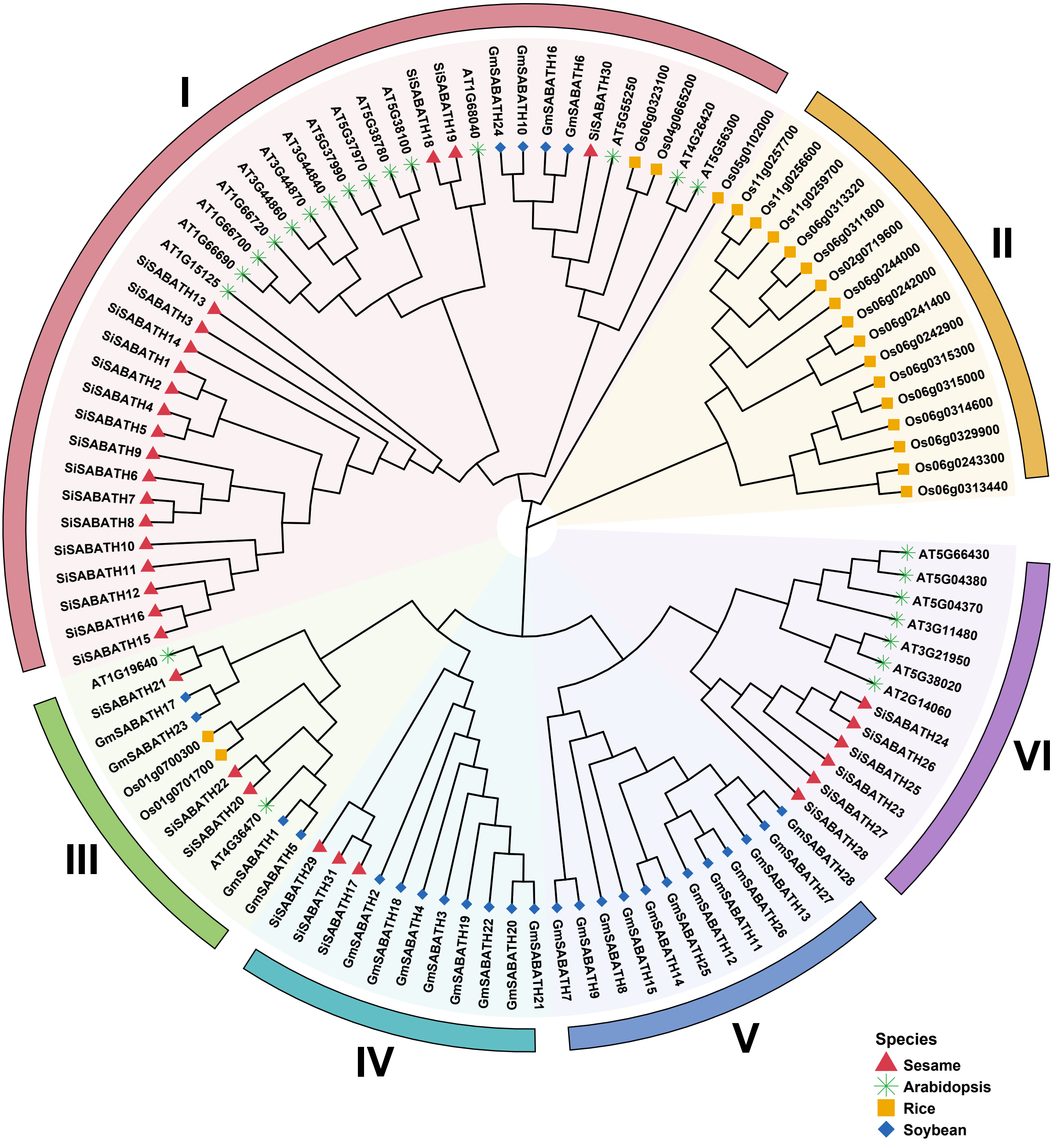
I
II
III
IV
V
VI
SiSABATH18
SiSABATH19
AT1G68040
GmSABATH24
GmSABATH10
GmSABATH16
GmSABATH6
SiSABATH30
AT5G55250
Os06g0323100
Os04g0665200
AT4G26420
AT5G56300
Os05g0102000
Os11g0257700
Os11g0256600
Os11g0259700
Os06g0313320
Os06g0311800
Os02g0719600
Os06g0244000
Os06g0242000
Os06g0241400
Os06g0242900
Os06g0315300
Os06g0315000
Os06g0314600
Os06g0329900
Os06g0243300
Os06g0313440
AT5G38100
AT5G38780
AT5G37970
AT5G37990
AT3G44840
AT3G44870
AT3G44860
AT1G66720
AT1G66700
AT1G66690
AT1G15125
SiSABATH13
SiSABATH3
SiSABATH14
SiSABATH1
SiSABATH2
SiSABATH4
SiSABATH5
SiSABATH9
SiSABATH6
SiSABATH7
SiSABATH8
SiSABATH10
SiSABATH11
SiSABATH12
SiSABATH16
SiSABATH15
AT5G66430
AT5G04380
AT5G04370
AT3G11480
AT3G21950
AT5G38020
AT2G14060
SiSABATH24
SiSABATH26
SiSABATH25
SiSABATH23
SiSABATH27
SiSABATH28
GmSABATH28
GmSABATH27
GmSABATH13
GmSABATH26
GmSABATH11
GmSABATH12
GmSABATH25
GmSABATH14
GmSABATH15
GmSABATH8
GmSABATH9
GmSABATH7
GmSABATH21
GmSABATH20
GmSABATH22
GmSABATH19
GmSABATH3
GmSABATH4
GmSABATH18
GmSABATH2
SiSABATH17
SiSABATH31
SiSABATH29
AT1G19640
SiSABATH21
GmSABATH17
GmSABATH23
Os01g0700300
Os01g0701700
SiSABATH22
SiSABATH20
AT4G36470
GmSABATH1
GmSABATH5
Species
Sesame
Arabidopsis
Rice
Soybean

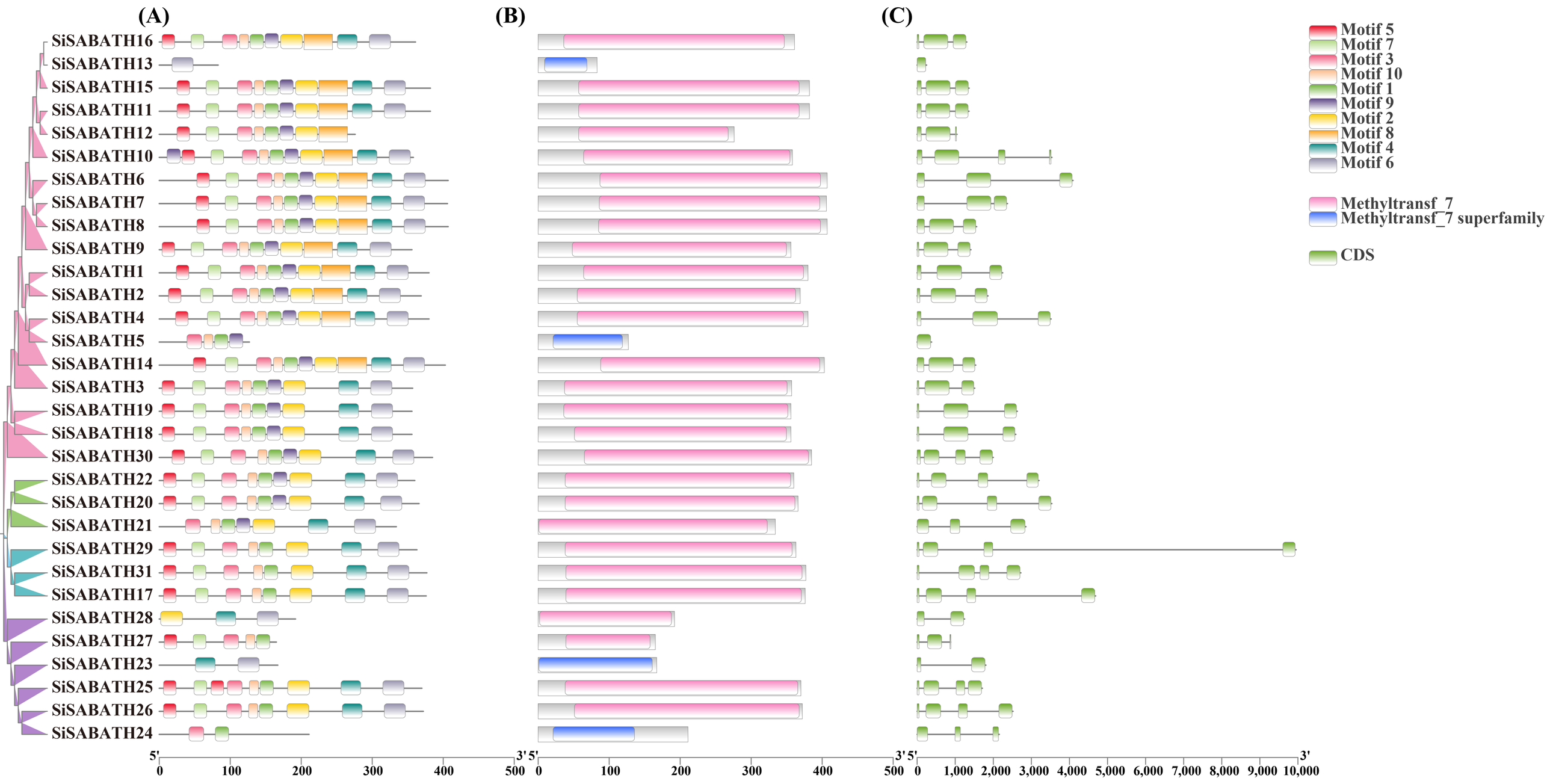
(A)
(B)
(C)
SiSABATH16
SiSABATH13
SiSABATH15
SiSABATH11
SiSABATH12
SiSABATH10
SiSABATH6
SiSABATH7
SiSABATH8
SiSABATH9
SiSABATH1
SiSABATH2
SiSABATH4
SiSABATH5
SiSABATH14
SiSABATH3
SiSABATH19
SiSABATH18
SiSABATH30
SiSABATH22
SiSABATH20
SiSABATH21
SiSABATH29
SiSABATH31
SiSABATH17
SiSABATH28
SiSABATH27
SiSABATH23
SiSABATH25
SiSABATH26
SiSABATH24
Motif 5
Motif 7
Motif 3
Motif 10
Motif 1
Motif 9
Motif 2
Motif 8
Motif 4
Motif 6
Methyltransf_7
Methyltransf_7 superfamily
CDS
5'
3'
0
100
200
300
400
500
1,000
2,000
3,000
4,000
5,000
6,000
7,000
8,000
9,000
10,000

	ARE	DRE core	LTR	MBS	MYB	MYC	STRE	TC−rich repeats	W box	WUN−motif	ABRE	as−1	CARE	CGTCA−motif	ERE	P−box	TCA−element	TGACG−motif	TGA−element	AuxRR−core	GARE−motif	A−box	AE−box	Box 4	CAT−box	circadian	GA−motif	GATA−motif	G−box	GTI−motif	I−box	MRE	RY−element	ACE	ATCT−motif	chs−CMA1a	L−box	Sp1	TCCC−motif	TCT−motif
SiSABATH1	2	0	0	1	2	7	1	0	0	1	5	3	0	3	0	0	0	3	0	0	0	1	0	6	0	0	0	0	5	4	0	0	0	0	0	0	1	0	1	2
SiSABATH2	0	0	0	2	4	3	1	0	1	0	5	2	0	2	2	1	0	2	0	0	0	0	0	1	0	0	1	2	6	0	0	0	0	0	0	0	0	0	0	0
SiSABATH3	1	2	1	1	2	3	2	0	0	0	4	4	0	4	0	0	0	4	1	0	0	2	1	1	3	0	0	0	6	0	1	0	0	0	0	0	0	1	2	2
SiSABATH4	1	0	1	0	1	6	3	0	0	2	7	0	0	0	1	0	0	0	1	0	0	0	0	5	0	0	1	1	8	0	0	2	0	0	1	1	0	0	1	1
SiSABATH5	2	0	2	0	3	9	2	0	0	1	1	1	0	1	1	0	3	1	1	1	0	0	0	3	1	1	0	4	1	1	0	0	0	0	0	0	0	0	0	1
SiSABATH6	1	0	0	1	4	4	2	0	2	0	3	1	0	1	0	0	0	1	1	0	0	0	1	4	0	1	0	1	2	2	0	0	0	0	0	1	0	0	0	2
SiSABATH7	0	0	0	1	5	7	0	1	0	0	0	0	0	0	3	0	0	0	0	0	0	0	2	8	0	0	0	0	1	3	1	0	1	0	0	0	0	0	0	0
SiSABATH8	3	0	1	0	2	4	4	0	2	1	4	1	0	1	1	1	0	1	0	0	1	0	0	3	0	0	1	0	6	0	1	0	0	0	0	1	0	0	1	0
SiSABATH9	2	0	2	3	5	4	0	0	1	0	5	2	0	2	0	0	2	2	0	0	0	0	0	5	0	0	1	0	6	1	1	0	0	0	0	0	0	0	1	2
SiSABATH10	2	1	0	0	1	4	0	0	0	2	1	0	0	0	2	1	0	0	1	1	0	0	0	4	0	0	0	1	1	1	1	0	0	0	0	0	0	0	1	1
SiSABATH11	3	0	1	1	5	2	0	0	1	0	1	1	0	1	4	0	0	1	1	0	1	0	0	2	0	0	0	0	1	2	0	0	0	1	1	0	0	0	0	1
SiSABATH12	3	0	1	0	4	1	0	0	1	0	0	1	0	1	4	0	0	1	1	0	1	0	0	2	0	0	0	0	1	1	0	0	0	1	1	0	0	0	0	1
SiSABATH13	3	0	4	1	8	0	1	0	1	1	2	2	1	2	0	0	0	2	1	1	1	0	0	2	0	0	0	1	1	1	1	0	0	0	0	0	0	0	0	0
SiSABATH14	2	0	0	2	6	9	1	0	1	2	4	1	0	1	1	0	2	1	0	0	2	0	0	3	0	0	0	0	3	1	0	1	0	1	0	0	0	0	0	0
SiSABATH15	2	1	0	1	7	3	1	0	2	0	0	1	0	1	3	0	0	1	1	0	2	0	0	6	0	0	0	0	0	0	0	0	0	0	0	0	0	0	0	1
SiSABATH16	1	0	1	2	3	3	2	0	1	1	2	2	0	2	3	0	0	2	1	0	0	0	1	2	0	0	0	0	2	1	0	0	0	1	0	0	0	0	0	0
SiSABATH17	2	0	0	0	4	5	1	1	0	0	0	1	0	1	4	1	0	1	0	0	1	0	0	1	2	1	0	0	1	3	0	0	0	0	0	0	0	0	0	2
SiSABATH18	0	0	0	1	8	7	0	0	1	1	4	2	0	2	1	0	0	2	1	0	0	0	0	5	1	1	0	1	6	2	1	0	0	0	0	1	0	0	1	0
SiSABATH19	0	0	0	0	2	3	0	0	1	0	5	1	0	1	3	0	1	1	1	0	0	0	0	6	0	0	1	1	5	0	0	0	0	0	0	0	0	1	0	
SiSABATH20	0	0	0	0	6	4	1	0	1	0	0	2	1	2	0	0	1	2	1	0	1	0	3	9	0	0	0	1	1	5	1	1	0	0	0	0	0	0	0	0
SiSABATH21	3	0	0	0	2	5	3	1	0	0	4	2	0	2	3	0	0	2	0	0	0	0	1	3	1	0	0	0	5	3	0	0	0	1	0	0	0	0	2	2
SiSABATH22	1	0	0	0	4	3	5	0	2	0	1	1	0	1	4	0	2	1	0	0	1	0	0	7	0	0	0	0	1	1	0	0	0	1	0	0	0	2	0	0
SiSABATH23	0	0	0	0	3	3	3	1	0	1	5	2	0	2	1	0	0	2	0	0	0	0	0	3	0	0	0	1	5	2	1	0	2	0	0	0	0	0	0	3
SiSABATH24	0	1	2	2	5	3	5	1	1	1	1	4	0	4	0	0	1	4	0	0	1	0	1	1	0	0	0	1	1	2	0	0	0	0	0	0	1	1	1	
SiSABATH25	1	0	1	0	3	3	3	0	0	2	0	2	0	2	0	0	1	2	0	0	0	1	0	1	0	1	0	1	0	0	0	0	0	0	0	0	0	2	1	
SiSABATH26	0	0	1	0	4	4	3	0	1	0	3	1	0	1	0	0	1	1	1	0	1	0	0	2	0	0	1	1	4	1	1	0	0	1	0	0	0	0	1	
SiSABATH27	0	0	1	0	3	8	1	2	1	1	7	2	0	2	2	0	0	2	0	0	0	0	1	3	0	0	0	0	9	2	0	0	0	1	0	0	0	0	0	2
SiSABATH28	1	0	0	1	5	5	3	0	0	2	2	3	0	3	1	2	0	3	0	0	1	0	0	1	0	0	0	1	3	0	0	0	0	1	0	0	0	0	0	1
SiSABATH29	1	0	1	3	4	4	0	0	0	0	2	1	0	1	2	0	1	1	0	0	0	1	1	8	0	0	0	0	3	3	0	0	0	0	0	0	0	0	0	0
SiSABATH30	3	0	0	1	4	4	2	0	0	2	1	0	0	0	2	0	0	0	0	0	0	1	0	5	0	0	2	1	1	1	0	1	1	0	1	1	0	2	0	0
SiSABATH31	0	1	0	0	3	2	1	0	2	2	3	1	0	1	2	0	2	1	0	0	0	0	0	6	1	0	1	2	3	3	0	0	1	1	0	0	0	0	0	1

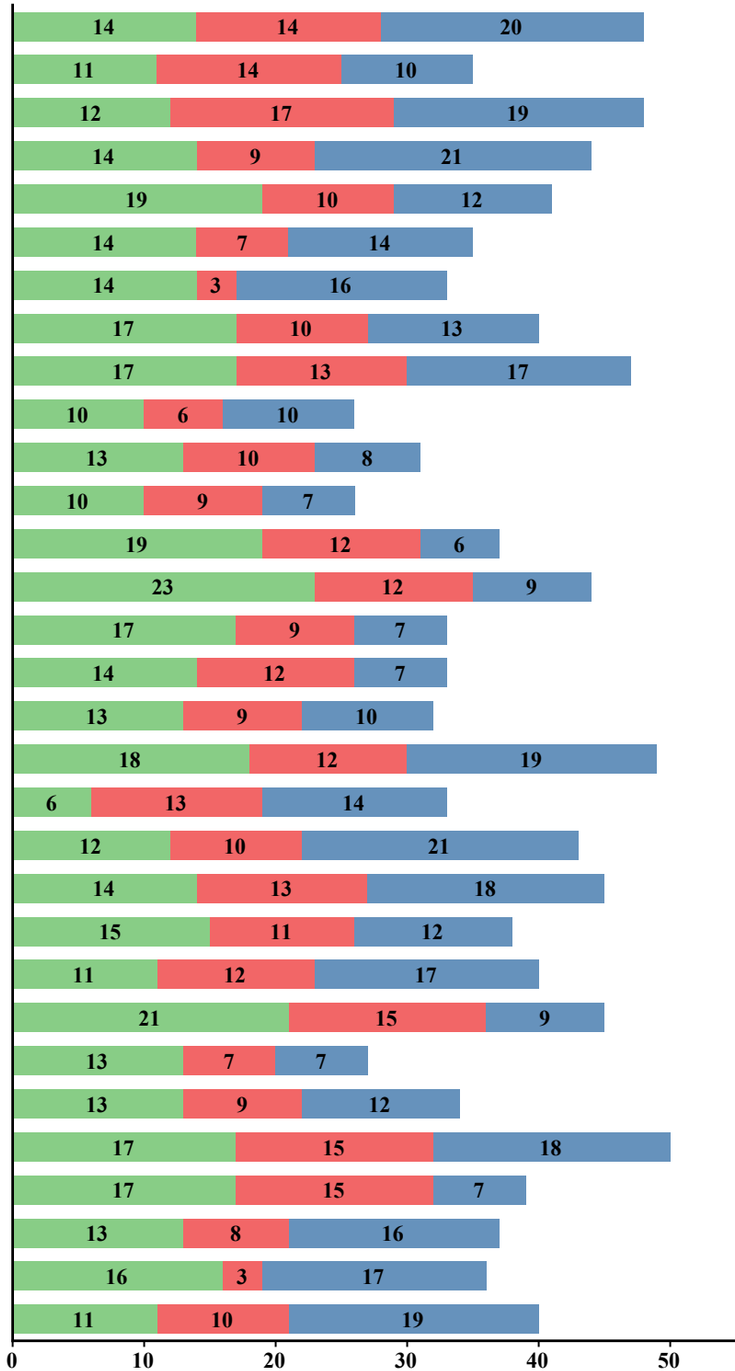

Abiotic and biotic stresses

Phytohormone responsive

Plant growth and development

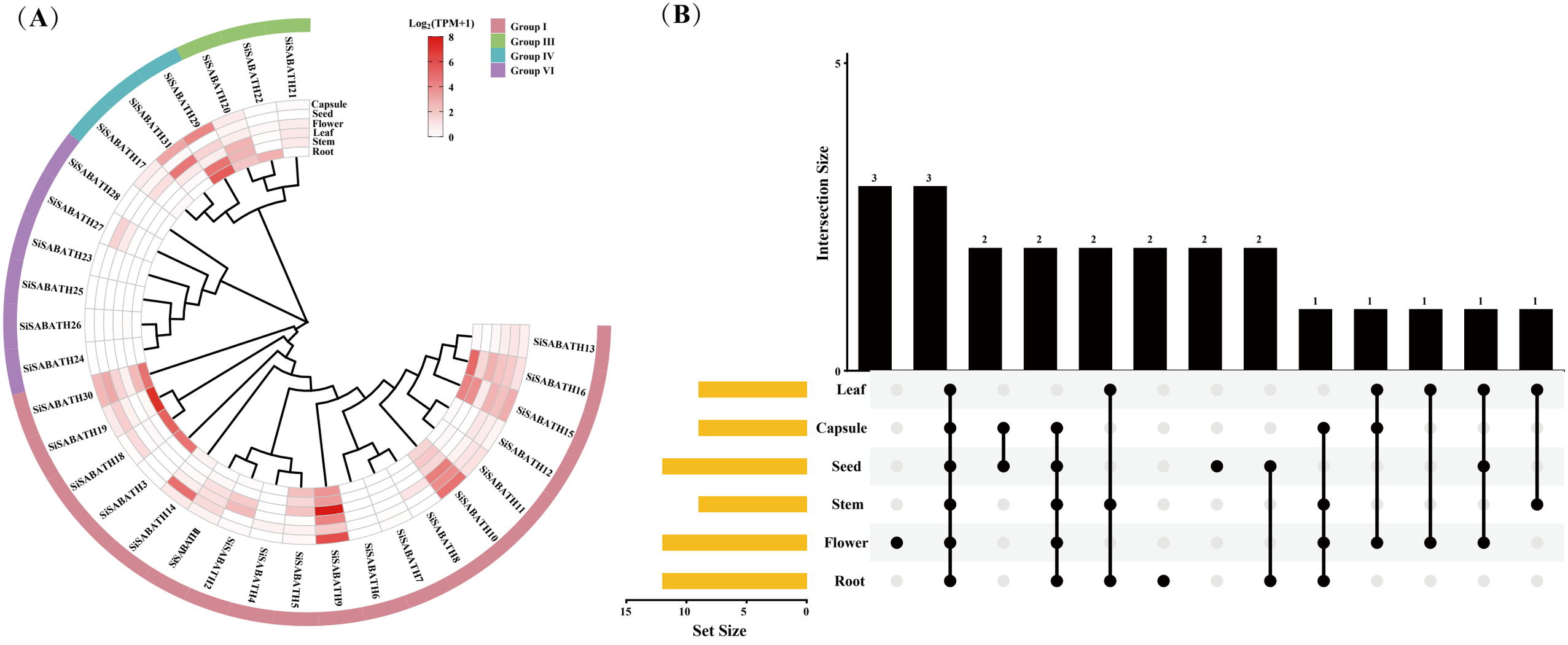
(A)
Log2(TPM+1)
8
6
4
2
0
Group I
Group III
Group IV
Group VI
SiSABATH21
SiSABATH22
SiSABATH20
SiSABATH29
SiSABATH31
SiSABATH17
SiSABATH28
SiSABATH27
SiSABATH23
SiSABATH25
SiSABATH26
SiSABATH24
SiSABATH30
SiSABATH19
SiSABATH18
SiSABATH3
SiSABATH14
SiSABATH13
SiSABATH2
SiSABATH4
SiSABATH5
SiSABATH9
SiSABATH6
SiSABATH7
SiSABATH8
SiSABATH10
SiSABATH11
SiSABATH12
SiSABATH15
SiSABATH16
Capsule
Seed
Flower
Leaf
Stem
Root
(B)
Intersection Size
5
0
3
3
2
2
2
2
2
2
1
1
1
1
1
Leaf
Capsule
Seed
Stem
Flower
Root
15
10
5
0
Set Size

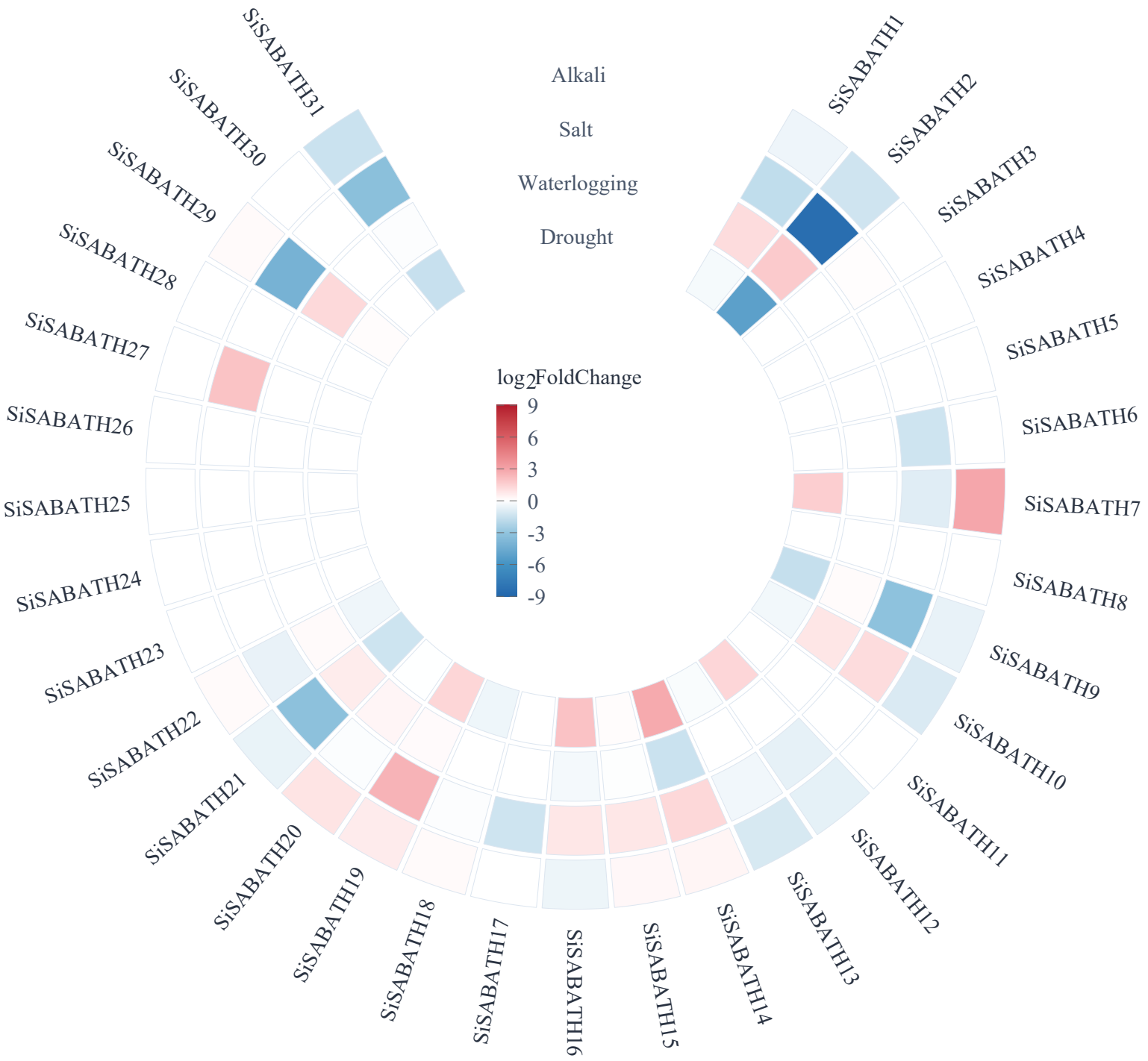
Alkali
Salt
Waterlogging
Drought
log2FoldChange
9
6
3
0
-3
-6
-9
SiSABATH1
SiSABATH2
SiSABATH3
SiSABATH4
SiSABATH5
SiSABATH6
SiSABATH7
SiSABATH8
SiSABATH9
SiSABATH10
SiSABATH11
SiSABATH12
SiSABATH13
SiSABATH14
SiSABATH15
SiSABATH16
SiSABATH17
SiSABATH18
SiSABATH19
SiSABATH20
SiSABATH21
SiSABATH22
SiSABATH23
SiSABATH24
SiSABATH25
SiSABATH26
SiSABATH27
SiSABATH28
SiSABATH29
SiSABATH30
SiSABATH31

SiSABATH16
SiSABATH15
SiSABATH12
SiSABATH11
SiSABATH10
SiSABATH9
SiSABATH6
SiSABATH7
SiSABATH8
SiSABATH1
SiSABATH2
SiSABATH4
SiSABATH5
SiSABATH14
SiSABATH3
SiSABATH13
SiSABATH19
SiSABATH18
SiSABATH30
SiSABATH22
SiSABATH20
SiSABATH21
SiSABATH31
SiSABATH17
SiSABATH29
SiSABATH26
SiSABATH24
SiSABATH25
SiSABATH23
SiSABATH27
SiSABATH28

Phylogenetic Group
Group I
Group III
Group IV
Group VI
Cold tolerance
Tolerant
Sensitive
Time
1 d
2 d
3 d
4 d
$\log_2$FC
6
3
0
−3
−6
|$\log_2$FC|
2
4
6

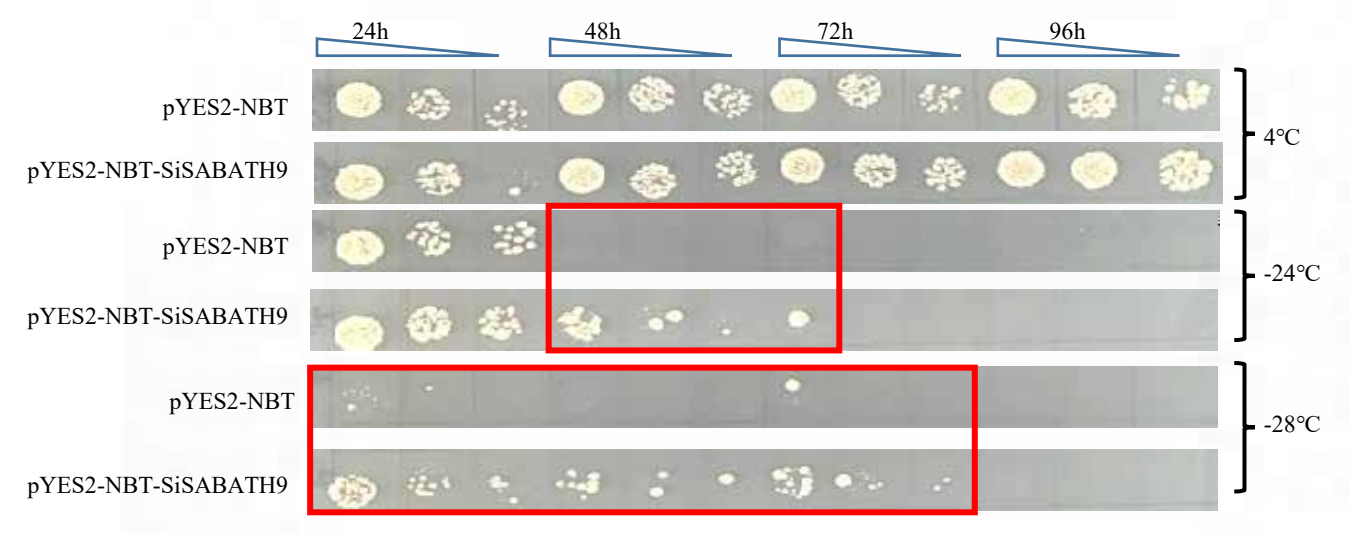
24h
48h
72h
96h
pYES2-NBT
pYES2-NBT-SiSABATH9
pYES2-NBT
pYES2-NBT-SiSABATH9
pYES2-NBT
pYES2-NBT-SiSABATH9
4°C
-24°C
-28°C

Supplementary Files

This is a list of supplementary files associated with this preprint. Click to download.

- Additionalfile1.docx
- Additionalfile2.xlsx